



Cite this: *Chem. Sci.*, 2021, **12**, 4825

All publication charges for this article have been paid for by the Royal Society of Chemistry

## Lithium silicate nanosheets with excellent capture capacity and kinetics with unprecedented stability for high-temperature CO<sub>2</sub> capture†

Rajesh Belgamwar,<sup>a</sup> Ayan Maity,<sup>a</sup> Tisita Das,<sup>d</sup> Sudip Chakraborty,<sup>b</sup> Chathakudath P. Vinod  <sup>c</sup> and Vivek Polshettiwar  <sup>a\*</sup>

An excessive amount of CO<sub>2</sub> is the leading cause of climate change, and hence, its reduction in the Earth's atmosphere is critical to stop further degradation of the environment. Although a large body of work has been carried out for post-combustion low-temperature CO<sub>2</sub> capture, there are very few high temperature pre-combustion CO<sub>2</sub> capture processes. Lithium silicate (Li<sub>4</sub>SiO<sub>4</sub>), one of the best known high-temperature CO<sub>2</sub> capture sorbents, has two main challenges, moderate capture kinetics and poor sorbent stability. In this work, we have designed and synthesized lithium silicate nanosheets (LSNs), which showed high CO<sub>2</sub> capture capacity (35.3 wt% CO<sub>2</sub> capture using 60% CO<sub>2</sub> feed gas, close to the theoretical value) with ultra-fast kinetics and enhanced stability at 650 °C. Due to the nanosheet morphology of the LSNs, they provided a good external surface for CO<sub>2</sub> adsorption at every Li-site, yielding excellent CO<sub>2</sub> capture capacity. The nanosheet morphology of the LSNs allowed efficient CO<sub>2</sub> diffusion to ensure reaction with the entire sheet as well as providing extremely fast CO<sub>2</sub> capture kinetics (0.22 g g<sup>-1</sup> min<sup>-1</sup>). Conventional lithium silicates are known to rapidly lose their capture capacity and kinetics within the first few cycles due to thick carbonate shell formation and also due to the sintering of sorbent particles; however, the LSNs were stable for at least 200 cycles without any loss in their capture capacity or kinetics. The LSNs neither formed a carbonate shell nor underwent sintering, allowing efficient adsorption–desorption cycling. We also proposed a new mechanism, a mixed-phase model, to explain the unique CO<sub>2</sub> capture behavior of the LSNs, using detailed (i) kinetics experiments for both adsorption and desorption steps, (ii) *in situ* diffuse reflectance infrared Fourier transform (DRIFT) spectroscopy measurements, (iii) depth-profiling X-ray photoelectron spectroscopy (XPS) of the sorbent after CO<sub>2</sub> capture and (iv) theoretical investigation through systematic electronic structure calculations within the framework of density functional theory (DFT) formalism.

Received 15th December 2020  
Accepted 15th February 2021

DOI: 10.1039/d0sc06843h  
[rsc.li/chemical-science](http://rsc.li/chemical-science)

## Introduction

Fossil fuels provide greater than 85% of the world's energy needs.<sup>1</sup> An excessive amount of CO<sub>2</sub> is the main cause of climate change. If the use of fossil fuel is to be continued in the coming years, the CO<sub>2</sub> emission needs to be dramatically reduced by developing sustainable sorbents to capture and separate CO<sub>2</sub> from various industrial processes. For CO<sub>2</sub> capture, in general, two protocols can be used, post-combustion and pre-

combustion.<sup>2–4</sup> Low-temperature sorbents (based on amines, silica, zeolites, carbon, and MOFs) are mainly used for post-combustion CO<sub>2</sub> capture from flue gas at low temperatures (25 to 75 °C), while high-temperature sorbents are specifically developed for pre-combustion capture between 500 and 700 °C.<sup>2–4</sup> "Pre-combustion capture" is one of the most challenging but best ways to tackle climate change as CO<sub>2</sub> is captured during the process at high temperatures with ideally zero release into the environment.<sup>5–7</sup> Pre-combustion capture is potentially less expensive than post-combustion capture, as CO<sub>2</sub> gets captured as soon as it is produced during the process without releasing it into the environment.<sup>5–7</sup>

Although a large body of work has been carried out for post-combustion low-temperature CO<sub>2</sub> capture,<sup>2</sup> there are very few high temperature pre-combustion CO<sub>2</sub> capture processes. Lithium silicate (Li<sub>4</sub>SiO<sub>4</sub>) is one of the best high-temperature CO<sub>2</sub> capture sorbents due to its relatively high capture capacities as compared to other alkali metal-containing ceramics.<sup>5–7</sup> Although lithium silicates display excellent CO<sub>2</sub> sorption

<sup>a</sup>Department of Chemical Sciences, Tata Institute of Fundamental Research (TIFR), Mumbai, India. E-mail: vivekpol@tifr.res.in

<sup>b</sup>Materials Theory for Energy Scavenging (MATES) Lab, Department of Physics, Indian Institute of Technology, Simrol, Indore, India

<sup>c</sup>Catalysis and Inorganic Chemistry Division, CSIR-National Chemical Laboratory (NCL), Pune, India

<sup>d</sup>Harish-Chandra Research Institute, HBNI, Allahabad, Uttar Pradesh, India

† Electronic supplementary information (ESI) available: Detailed experimental, the effect of mole ratio, the effect of thermal treatment temperature and time, the effect of CO<sub>2</sub> flow, XPS data, and kinetic data. See DOI: 10.1039/d0sc06843h



capabilities at high temperatures, they face two main limitations, slow capture kinetics and poor stability-recyclability of the sorbents.<sup>5-7</sup> Formation of a lithium carbonate product layer limits  $\text{CO}_2$  diffusion, thus limiting kinetic performance; second, sintering reduces the cycling stability necessary for practical application. Recently, nanowires of lithium silicates and lithium tungstate showed good kinetics of  $\text{CO}_2$  capture.<sup>8,9</sup> However, these nanowires were not stable against agglomeration/sintering during the high-temperature  $\text{CO}_2$  adsorption-

desorption process, with a loss of 50% of their capture performance (capacity and kinetics) in the first three cycles. Thus, there was a need for a sorbent that has the following properties: (i) high  $\text{CO}_2$  capture at elevated temperatures (between 600 and 750 °C), (ii) faster rate of adsorption/desorption, and (iii) cycling stability for hundreds of  $\text{CO}_2$  capture-release cycles.

In continuation of our work on  $\text{CO}_2$  capture and conversion,<sup>10-13</sup> here we report lithium silicate nanosheets (LSNs) as a high-temperature  $\text{CO}_2$  sorbent. The LSNs showed a high  $\text{CO}_2$

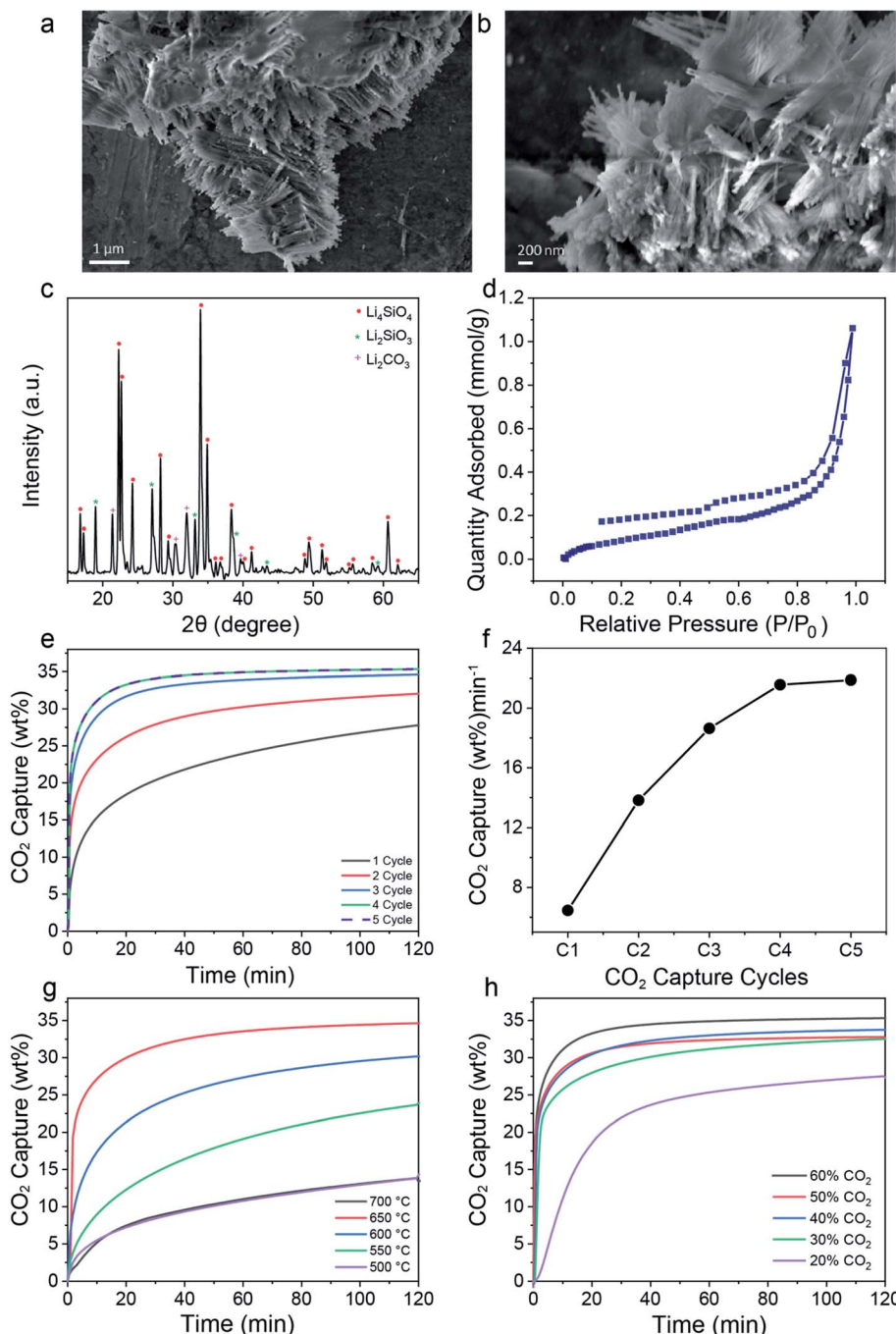


Fig. 1 (a and b) SEM images, (c) PXRD pattern, and (d)  $\text{N}_2$  sorption isotherm of the LSNs; (e)  $\text{CO}_2$  adsorption thermograms, (f)  $\text{CO}_2$  capture kinetics in the first minute at 650 °C using 60%  $\text{CO}_2$  for various cycles; (g)  $\text{CO}_2$  capture by the LSNs (4-cycle activated) at various temperatures; (h)  $\text{CO}_2$  capture capacity at 650 °C for feeds with various  $\text{CO}_2$  concentrations.

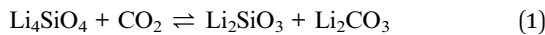


capture capacity of 35.3 wt% CO<sub>2</sub> (96.18% efficiency, in comparison with the theoretical capacity of 36.7 wt%) and ultra-fast kinetics (0.22 g g<sup>-1</sup> min<sup>-1</sup>). Notably, the LSNs were stable even after 200 cycles without any loss in their capture capacity or kinetics.

## Results and discussion

LSNs were synthesized using dendritic fibrous nanosilica (DFNS).<sup>12</sup> The DFNS surface area is highly accessible by virtue of its fibrous nature instead of tubular pores like in MCM-41 and SBA-15.<sup>12</sup> After several synthetic optimizations, in terms of lithium precursor, heating temperature and time (Tables S1 to S3†), the desired LSNs were prepared by thermal treatment of physically mixed DFNS and lithium nitrate with a Li : Si molar ratio of 4.66 : 1 at 650 °C for 6 h in air. Scanning electron microscopy (SEM) images indicated that the LSNs are made up of nanosheets randomly stacked on each other with overall sheet widths of a few microns (Fig. 1a and b). Powder X-ray diffraction (PXRD) of the LSNs showed the presence of Li<sub>4</sub>SiO<sub>4</sub> as a major phase, with Li<sub>2</sub>SiO<sub>3</sub> and Li<sub>2</sub>CO<sub>3</sub> as minor phases (Fig. 1c). These impurities were due to the reaction of the LSNs with trace amounts of CO<sub>2</sub> present (~400 ppm) in the environment during LSN synthesis. Synthesis of the pure phase of Li<sub>4</sub>SiO<sub>4</sub> was possible by using an inert atmosphere (Fig. S1†); however, since a small amount of minor phases did not affect the CO<sub>2</sub> performance of the LSNs, we chose sustainable synthesis conditions in an air environment. The N<sub>2</sub> sorption isotherm (Fig. 1d) displayed type IV characteristics with hysteresis and a low surface area of 8 m<sup>2</sup> g<sup>-1</sup>.

The CO<sub>2</sub> capture performance of the LSNs was evaluated using thermogravimetric analysis (TGA). First, the CO<sub>2</sub> adsorption/desorption of the LSNs was studied at 650 °C using 60% CO<sub>2</sub> (balance nitrogen) with 25 mg of sorbent (Fig. 1e and f, and S2† for the effect of sorbent weight). Notably, we observed an increase in capture capacity from 0.277 to 0.353 g g<sup>-1</sup> as well as initial kinetics from 0.06 to 0.22 g g<sup>-1</sup> min<sup>-1</sup> up to the 4<sup>th</sup> cycle. The increase in capture capacity and kinetics up to the 4<sup>th</sup> cycle was due to systematic purification of the as-prepared Li<sub>4</sub>SiO<sub>4</sub>, which had Li<sub>2</sub>SiO<sub>3</sub>, and Li<sub>2</sub>CO<sub>3</sub> as minor phases. With every cycle of CO<sub>2</sub> adsorption–desorption, these minor phases were converted to Li<sub>4</sub>SiO<sub>4</sub> and at the 4<sup>th</sup> cycle, their concentrations were significantly reduced (Fig. 2a). The PXRD pattern indicated the reaction of Li<sub>4</sub>SiO<sub>4</sub> with CO<sub>2</sub> to form Li<sub>2</sub>SiO<sub>3</sub> and Li<sub>2</sub>CO<sub>3</sub> during the adsorption step followed by the conversion of Li<sub>2</sub>SiO<sub>3</sub> and Li<sub>2</sub>CO<sub>3</sub> phases to Li<sub>4</sub>SiO<sub>4</sub> during the CO<sub>2</sub> desorption step (eqn (1)). This process was reversible (Fig. 2a), which was the reason for the better cycling stability of the LSNs.



The LSNs' CO<sub>2</sub> capture performance was then studied at different temperatures using a 4-cycle activated sample using 60% CO<sub>2</sub> with 25 mg of sorbent (Fig. 1g). The CO<sub>2</sub> sorption capacity first increased from 500 to 650 °C and then decreased

at 700 °C. At 500 °C, the diffusion process was kinetically controlled, and the diffusion barrier is the main reason for the low CO<sub>2</sub> sorption capacity. With the increase in temperature to 650 °C, the diffusion and chemisorption processes were accelerated and hence the CO<sub>2</sub> capture rate was much faster. However, at 700 °C, the desorption kinetics of CO<sub>2</sub> was faster than the adsorption kinetics, reducing the overall capture capacity and kinetics. Thus, 650 °C was found to be the optimized temperature in terms of CO<sub>2</sub> capture capacity. At this temperature, using these 4-cycle activated LSNs, the effect of CO<sub>2</sub> concentration was also studied, with 20, 30, 40, 50 and 60% CO<sub>2</sub>, all of which (except 20% CO<sub>2</sub>) showed good capture capacities and kinetics (Fig. 1h and S3†), indicating their usability in various pre-combustion processes where different amounts of CO<sub>2</sub> are generated. We then studied the effect of gas flow using 150, 100, and 50 mL min<sup>-1</sup> of 100% CO<sub>2</sub> (Fig. S4†). The LSNs showed good capture rates with all the flows, indicating their usability in various processes with different flows.

X-ray photoelectron spectroscopy (XPS) was performed to study the LSNs and how they change during CO<sub>2</sub> adsorption–desorption steps (Fig. 2b). The XPS spectra contained two peaks for Li (1s) at binding energies (BEs) of ~54 eV and ~55.9 eV. The peak at ~54 eV was assigned to Li<sub>4</sub>SiO<sub>4</sub> (major phase)<sup>14</sup> as well as Li<sub>2</sub>CO<sub>3</sub> (minor phase).<sup>15</sup> Although their deconvolution was not possible due to their very close binding energy (BE), based on PXRD, this peak at ~54 eV was assigned mainly to Li<sub>4</sub>SiO<sub>4</sub>. The signal at ~55.9 eV was assigned to Li<sub>2</sub>SiO<sub>3</sub>.<sup>14,15</sup> After CO<sub>2</sub> capture, in the adsorbed 4-cycle activated sample, the area under the peak of Li<sub>2</sub>SiO<sub>3</sub> at ~55.9 eV increased due to the conversion of Li<sub>4</sub>SiO<sub>4</sub> to Li<sub>2</sub>SiO<sub>3</sub> and Li<sub>2</sub>CO<sub>3</sub>, as also observed in PXRD (Fig. 2a). The formation of Li<sub>2</sub>CO<sub>3</sub> was observed with the signal at ~54 eV BE (overlapping with the Li<sub>4</sub>SiO<sub>4</sub> signal), but clearly differentiable in PXRD. The Si (2p) spectra of the LSNs showed two Si signals, at BEs of ~101 eV for Li<sub>4</sub>SiO<sub>4</sub> and ~102 eV for Li<sub>2</sub>SiO<sub>3</sub> (Fig. 2a).<sup>14,15</sup> After CO<sub>2</sub> adsorption, ideally, there should be only one Si site, as PXRD indicates the presence of Li<sub>2</sub>SiO<sub>3</sub> and Li<sub>2</sub>CO<sub>3</sub> only (Fig. 2a). However, we observed two signals, at ~102 and ~104 eV. This indicates that the signal at ~104 eV was for SiO<sub>2</sub>.<sup>16</sup>

The LSNs' stability and cyclability were then studied and the results indicated that the LSNs could be used for at least 200 cycles without any loss in their capture capacity or kinetics (Fig. 3a). We compared the recyclability of the LSNs with that of the best lithium silicates reported in the literature (Fig. 3b and Table S4†). The LSNs were found to be stable and did not lose their capture capacity or kinetics during the adsorption–desorption cycling. In general, conventional lithium silicates systematically lose their capture capacity with every cycle with a significant loss in the first few cycles (Fig. 3b);<sup>5–7,17–29</sup> however, the LSNs were found to be stable even after 200 cycles. The LSNs were even better than one of the best recently reported sorbents, lithium silicate nanowires (NWs)<sup>8</sup> (Fig. 3c). The NW sorbent lost more than 50% of its capture capacity, which fell from 0.35 to 0.15 g g<sup>-1</sup>, in just four cycles, while the LSNs capture capacity (0.35 g g<sup>-1</sup>) did not change even after 200 cycles. The kinetics of the NWs reduced to 0.1 g g<sup>-1</sup> min<sup>-1</sup> in 4 cycles, while the LSNs kinetics remained at 0.22 g g<sup>-1</sup>



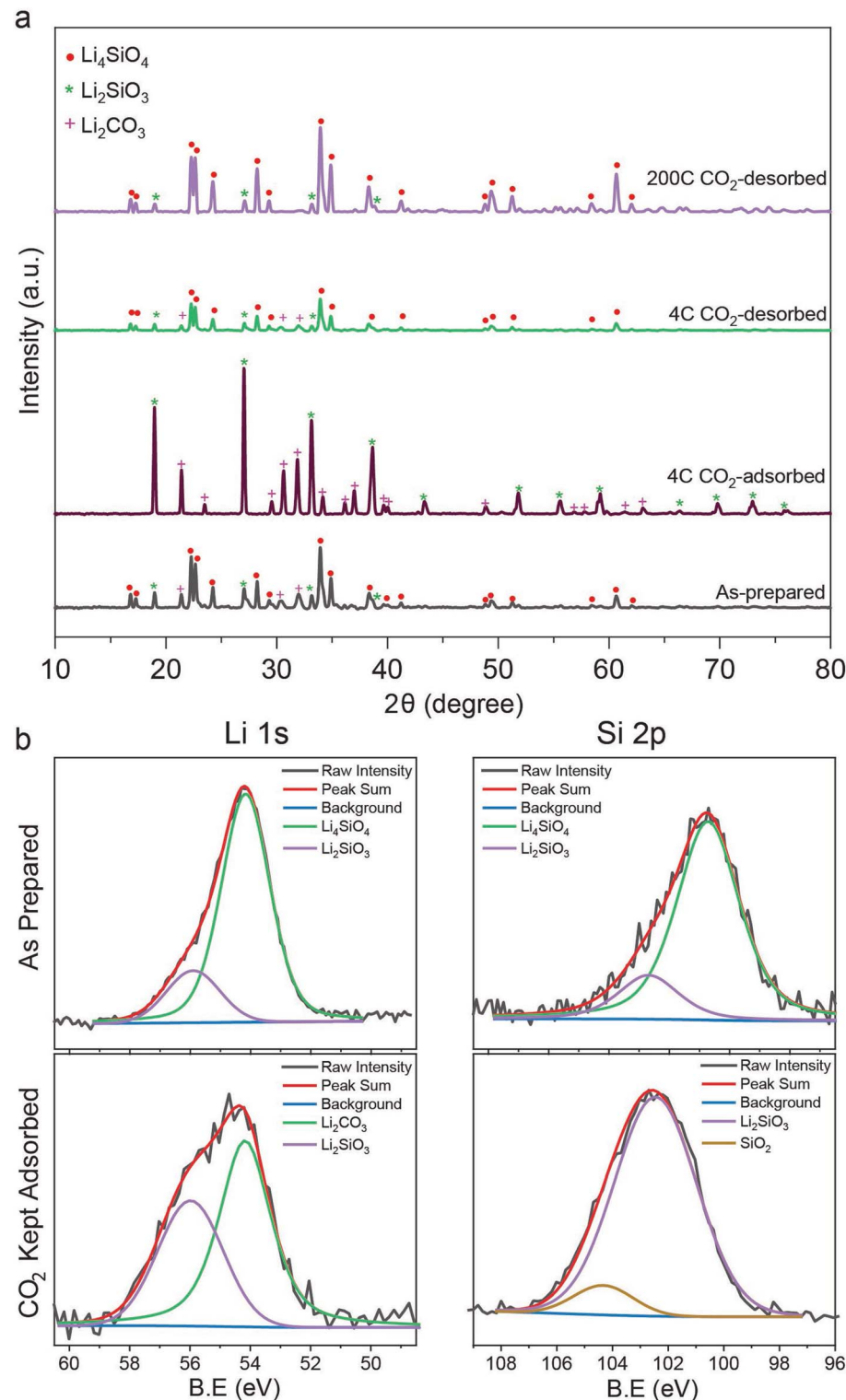


Fig. 2 (a) PXRD pattern and (b) XPS spectra of lithium silicates after various  $\text{CO}_2$  adsorption–desorption cycles.

$\text{min}^{-1}$  even after 200 cycles. Thus, we found that the LSNs outperform the NWs and other reported sorbents in terms of capture capacity and kinetics as well as cycling stability. Notably, the LSNs were even stable in the presence of a  $\text{CO}_2$  feed containing water vapor (Fig. S5†).

For most of the reported  $\text{Li}_4\text{SiO}_4$ , due to its dense morphology and large particle size (Table S4†),  $\text{CO}_2$  capture took place mainly at the surface, while the interior surface cannot fully interact with  $\text{CO}_2$ , which limits the capture capacity of the conventional lithium silicate material. Also, as pore size

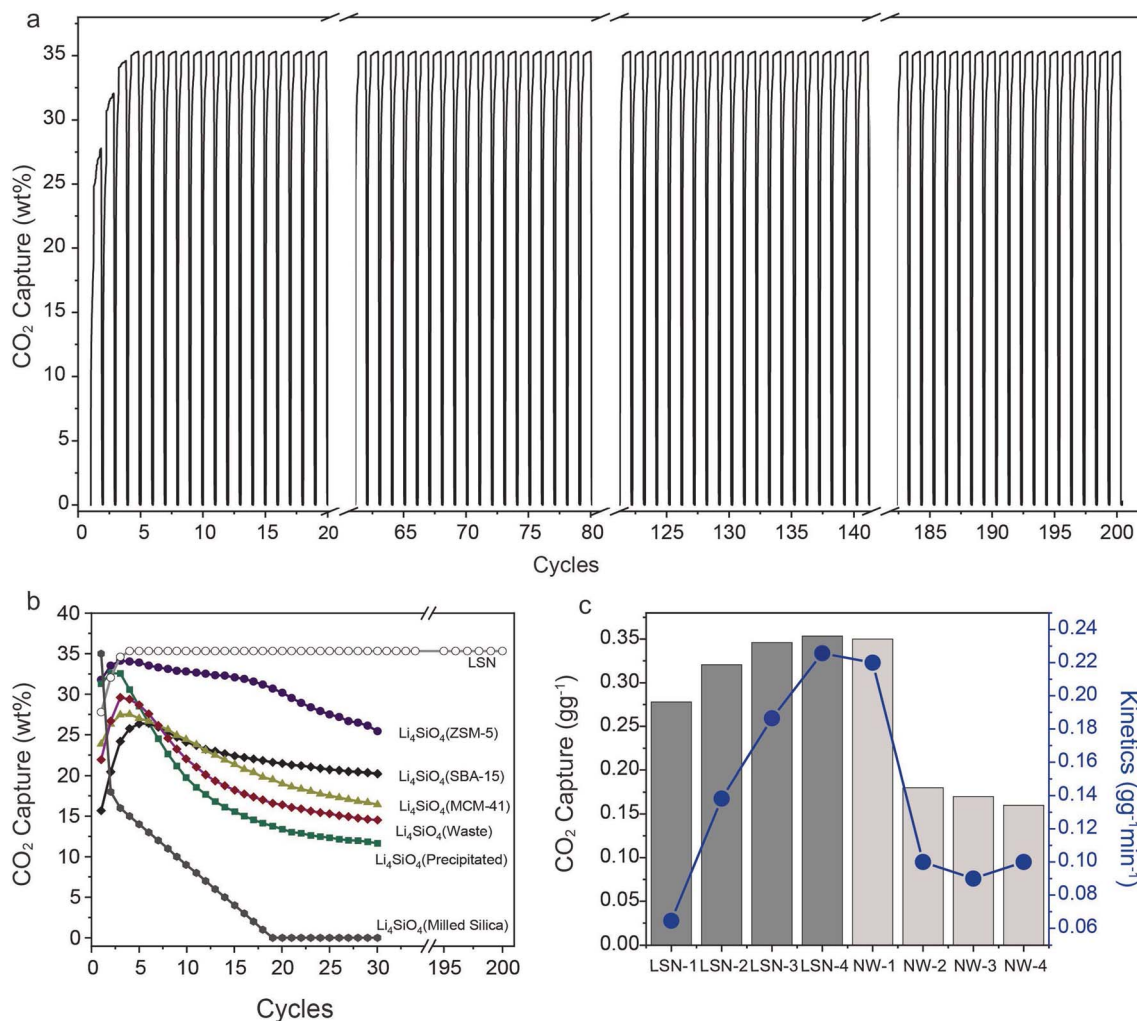


Fig. 3 (a) Stability and cyclability of the LSNs for 200 cycles of CO<sub>2</sub> adsorption–desorption, (b) comparison with various best-known lithium silicate sorbents, and (c) cycle-by-cycle comparison of the LSNs with lithium silicate nanowires (NWs)<sup>8</sup> at 650 °C using 60% CO<sub>2</sub>.

has a critical impact on the CO<sub>2</sub> capture performance of Li<sub>4</sub>SiO<sub>4</sub>,<sup>5</sup> due to the formation of Li<sub>2</sub>SiO<sub>3</sub> and Li<sub>2</sub>CO<sub>3</sub>, which have a higher molar volume than Li<sub>4</sub>SiO<sub>4</sub>, the pores get blocked due to this volumetric expansion, causing further degradation in the sorbent's CO<sub>2</sub> capture performance (capacity, kinetics, and recyclability). Our synthesized sorbent LSNs, due to their thin sheets, provided a good external surface and allowed CO<sub>2</sub> diffusion to every Li-site without any hindrance. Although the LSNs aggregated after 4 cycles, these sheets did not undergo

sintering even after 200 cycles, possibly because they were covalently interlinked with each other between the sheets (Fig. S6 and S7†), and remained stable for 200 cycles. This was the reason for the excellent CO<sub>2</sub> sorption performance of this sorbent (with CO<sub>2</sub> capture capacity close to the theoretical value).

According to the double-shell model<sup>5</sup> (Fig. 4, left), first Li<sub>4</sub>SiO<sub>4</sub> reacts with CO<sub>2</sub> at the sorbent surface to generate an external shell made up of Li<sub>2</sub>CO<sub>3</sub>. Once this shell is formed, the

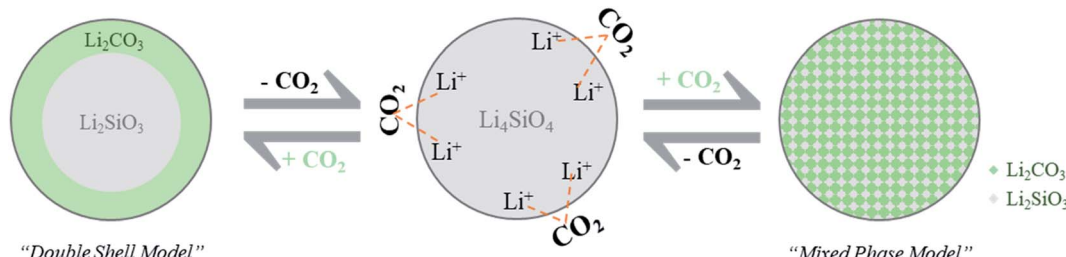


Fig. 4 Proposed mixed-phase vs. double shell model for CO<sub>2</sub> adsorption–desorption.

diffusion of  $\text{CO}_2$  and  $\text{Li}^+$  through this external shell dictates the sorbent performance. The formation of thick carbonate shells was the main reason for the degradation of capture performance for the conventional lithium silicates.<sup>5</sup> In the case of the LSNs, the sheet thickness is a few nanometers, and hence  $\text{CO}_2$  and  $\text{Li}^+$  can easily diffuse across the entire sheet, and  $\text{CO}_2$  reacts with  $\text{Li}^+$  without the formation of the external shell. The rate of the  $\text{CO}_2$  capture is generally limited by the diffusion of  $\text{CO}_2$  and  $\text{Li}^+$  through the external shell; however, since no such shell was formed in the LSNs, they showed extremely fast  $\text{CO}_2$  capture kinetics ( $0.22 \text{ g g}^{-1} \text{ min}^{-1}$ ). Based on these observations, we propose that the LSNs adsorb/desorb  $\text{CO}_2$  via a mixed-phase model and not the double-shell model (Fig. 4).

To study this process and understand the effect on  $\text{CO}_2$  chemisorption and  $\text{Li}^+$  diffusion, isotherms at different temperatures were fitted to the double-exponential equation (eqn (2); Fig. S8†)

$$y = A \exp(-k_1 x) + B \exp(-k_2 x) + C \quad (2)$$

**Table 1** Kinetic parameters obtained from the LSNs' adsorption isotherms at different temperatures

T (°C)	$k_1 (\text{s}^{-1})$	$k_2 (\text{s}^{-1})$	$R^2$
500	0.003510	0.00093	0.99878
550	0.003783	0.00028	0.99943
600	0.006214	0.00048	0.99771
650	0.065421	0.00164	0.99068
700	0.001788	0.00015	0.99960

where  $y$  represents the  $\text{CO}_2$  adsorbed in wt%,  $x$  is the time required to capture  $\text{CO}_2$ , and  $k_1$  and  $k_2$  are the exponential parameters for  $\text{CO}_2$  chemisorption and lithium diffusion processes, respectively.  $A$  and  $B$  are constants, and  $C$  is the  $y$ -axis intercept.

Table 1 summarizes the kinetic parameters obtained after this fitting from the LSNs'  $\text{CO}_2$  adsorption isotherms (Fig. S4†). At the optimized sorption temperature, 650 °C,  $k_1$  was  $0.065421 \text{ s}^{-1}$ , far better than the reported values for conventional silicates,<sup>5–7</sup> indicating extremely fast  $\text{CO}_2$  chemisorption by interaction with  $\text{Li}^+$  ions on the surface of the LSNs (Fig. 4). This confirms the role of nanosheet morphology, which allowed more external surface and less core, causing efficient  $\text{CO}_2$  adsorption and indicating the mixed-phase model of  $\text{CO}_2$  capture. In conventional silicates, in the 2<sup>nd</sup> step, the  $\text{Li}^+$  ion has to diffuse through carbonate shells (as per the double-shell model, Fig. 4), and this slows down the  $\text{CO}_2$  capture kinetics ( $k_2$ ). In the case of LSNs,  $k_2$  was  $0.00164 \text{ s}^{-1}$ , similar to reported values. However, in the case of LSNs, more than 90% of the total  $\text{CO}_2$  capture happened in the first 3 minutes, indicating that  $k_1$  ( $\text{CO}_2$  chemisorption) is the rate-limiting step and not  $k_2$  ( $\text{Li}^+$  diffusion). This again indicates that the LSNs'  $\text{CO}_2$  capture follows the proposed mixed-phase model.

In order to gain more insight into the mixed-phase model, we compared the LSN sorbent (prepared from DFNS) with a conventional sorbent prepared from Stöber silica, named Stöber lithium silicate (SLS), which is known to follow the double-shell model of  $\text{CO}_2$  adsorption–desorption. When we

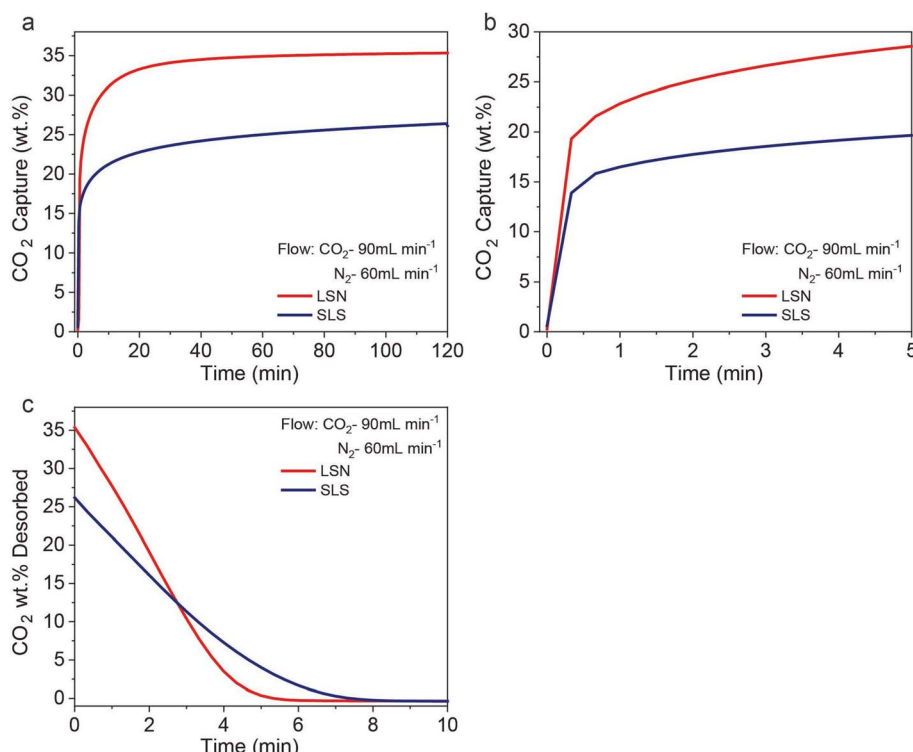


**Fig. 5**  $\text{CO}_2$  capture by the LSNs and SLS at 650 °C using 60%  $\text{CO}_2$ : (a)  $\text{CO}_2$  adsorption thermograms of the LSNs and SLS; (b)  $\text{CO}_2$  capture kinetics in the first five minutes; (c)  $\text{CO}_2$  desorption kinetics.



compared the  $\text{CO}_2$  capture performance of the LSNs and SLS using feed with various  $\text{CO}_2$  concentrations, in all cases, the LSNs showed far better  $\text{CO}_2$  capture capacity and kinetics as compared to SLS (Fig. S9†). For further comparison, we chose a feed with a 60 : 40 ratio of  $\text{CO}_2 : \text{N}_2$  and observed that in 2 h, the LSNs capture 35.3 wt%  $\text{CO}_2$  (22.04 wt% in the first minute) while SLS captures only 26.2 wt% (16.49 wt% in the first minute) (Fig. 5a). The LSNs showed faster kinetics of 5.8 wt% per minute, compared to the 3.1 wt% per minute for SLS (Fig. 5b), indicating faster Li diffusion throughout the LSNs, supporting the mixed-phase model. This model should also significantly affect desorption kinetics, as kinetics should be faster in the case of a mixed-phase model compared to the double-shell model, which is known for slow desorption due to the thick shell. The LSNs showed very fast desorption, 6.8 wt% per minute, while SLS desorbed 5.1 wt% per minute with respect to their total capture capacity. A similar trend was observed under all three flow conditions (Fig. S10†). This confirms the presence of a mixed-phase model in the LSNs but the double-shell model in SLS.

If the proposed mixed-phase model is correct,  $\text{CO}_2$  chemisorption should be a rate-determining step and not lithium-ion diffusion. The extremely high value of  $k_1$  and low value of  $k_2$  (in Table 1) clearly indicate that chemisorption is a major path of  $\text{CO}_2$  adsorption, while the lithium-ion diffusion path is insignificant. We then fitted the adsorption kinetics to a single

exponential equation (eqn (S1)†) and found that  $k_1$  was  $0.00285 \text{ s}^{-1}$  for the LSNs and  $0.00093 \text{ s}^{-1}$  for SLS (Fig. S11 and Table S5†). In addition to adsorption kinetics, desorption kinetics should also be accelerated by the mixed-phase model. We hence fitted the desorption (Fig. 5c) to the single exponential equation (Fig. S12†) and found that  $k_1$  was  $0.002027 \text{ s}^{-1}$  for the LSNs as compared to only  $0.001652 \text{ s}^{-1}$  for SLS. This also confirms the presence of a mixed-phase model in the case of LSNs.

To gain mechanistic insights into the  $\text{CO}_2$  capture process of  $\text{CO}_2$  adsorption on the  $\text{Li}_4\text{SiO}_4$  surface and the formation of  $\text{Li}_2\text{CO}_3$  and  $\text{Li}_2\text{SiO}_3$ , we carried out *in situ* diffuse reflectance infrared Fourier transform (DRIFT) spectroscopy measurements of the LSNs under similar  $\text{CO}_2$  adsorption and desorption conditions. For the adsorption study, in a reactor chamber with a heater and gas flow controller, the LSNs were treated with  $\text{CO}_2$  (60%) at  $650^\circ\text{C}$ , while for the desorption study, the LSNs, after  $\text{CO}_2$  treatment, were treated with  $\text{N}_2$  at  $650^\circ\text{C}$  and an IR spectrum was recorded at various time intervals. The band at  $2342 \text{ cm}^{-1}$  was assigned to the linearly chemisorbed  $\text{CO}_2$  molecule on the lithium silicate surface (Fig. S13a and b†),<sup>30</sup> while the band in the region of  $3500$  to  $3900 \text{ cm}^{-1}$  was assigned to  $\text{Si-OH}^{10}$  of lithium silicates (Fig. S13c and d†).

The intensity of the band in the region of  $650$ – $750 \text{ cm}^{-1}$ , assigned to the stretching vibration of  $\text{Si-O-Si}$  of the  $\text{SiO}_3$  chain present in  $\text{Li}_2\text{SiO}_3$  (ref. 31), increased with time (Fig. 6a) as the LSNs on exposure to  $\text{CO}_2$  (adsorption step) converted to  $\text{Li}_2\text{SiO}_3$

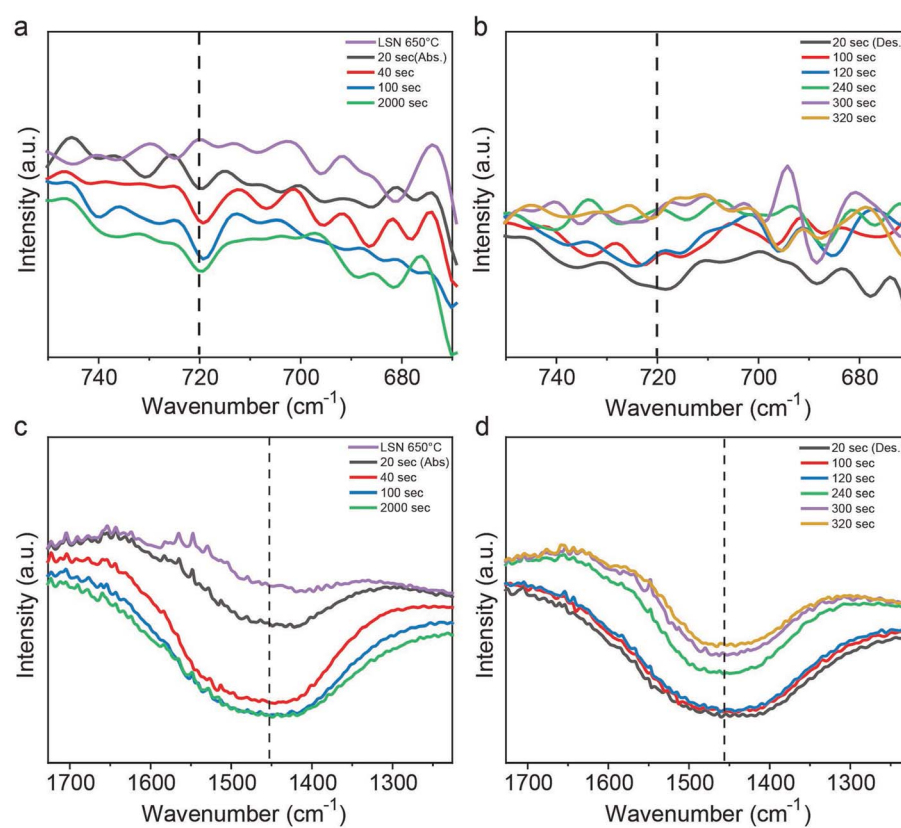


Fig. 6 *In situ* DRIFT study of  $\text{CO}_2$  adsorption–desorption using the LSNs and SLS at  $650^\circ\text{C}$ . FTIR spectra of LSN (a and b) adsorption and (c and d) desorption steps. Adsorption is by 60%  $\text{CO}_2$  while desorption is by 100%  $\text{N}_2$ .



and  $\text{Li}_2\text{CO}_3$ . When  $\text{CO}_2$  was replaced by a  $\text{N}_2$  flow (desorption step), the intensity of these bands decreased with time (Fig. 6b), indicating that  $\text{Li}_2\text{SiO}_3$  and  $\text{Li}_2\text{CO}_3$  converted back into  $\text{Li}_4\text{SiO}_4$ . The desorption took place in just 240 s (4 minutes), and such fast desorption indicates the mixed-phase model, as the double-shell model had very slow desorption kinetics. Along similar lines, the intensity of the band in the region of  $1300\text{--}1600\text{ cm}^{-1}$ , assigned to the stretching vibration of C–O in the carbonate ion ( $\text{CO}_3^{2-}$ ) present in  $\text{Li}_2\text{CO}_3$  (ref. <sup>32</sup>), increased with time (Fig. 6c) as the LSNs on exposure to  $\text{CO}_2$  (adsorption step) converted to  $\text{Li}_2\text{SiO}_3$  and  $\text{Li}_2\text{CO}_3$ . During the desorption (Fig. 6d), this signal intensity decreased with time. Since complete disappearance was not observed, the as-synthesized LSNs have the impurity of lithium carbonate.

To further study the proposed mixed-phase model of  $\text{CO}_2$  adsorption–desorption, an XPS depth-profiling study of the LSNs was carried out by etching at various depths of the LSN sample after the  $\text{CO}_2$  adsorption step (Fig. 7). If it is a conventional double-shell model, one should see lithium carbonate only at the surface (and not in the core) in XPS, while if it is the proposed mixed-phase model, lithium carbonate should be present at the surface as well as inside the core. The XPS depth profile of the LSN sample after  $\text{CO}_2$  adsorption is shown in Fig. S14.† We calculated the area under the peak for Li 1s corresponding to  $\text{Li}_2\text{SiO}_3$  and  $\text{Li}_2\text{CO}_3$  (Fig. 7a) and observed that at all depths from 0 to 255 nm, there was a presence of both  $\text{Li}_2\text{CO}_3$  and  $\text{Li}_2\text{SiO}_3$ , clearly confirming the mixed-phase model. This was further confirmed by comparing the area under the

peak for Si 2p and C 1s at various depths (Fig. 7b and c) and notably, Si 2p and C 1s also followed the same trend as Li 1s, confirming the presence of  $\text{Li}_2\text{CO}_3$  and  $\text{Li}_2\text{SiO}_3$  across the LSNs. This further supports the proposed mixed-phase model of  $\text{CO}_2$  adsorption and desorption by the LSNs.

In order to gain further insight into the adsorption/desorption kinetics of the LSN sorbent, a theoretical investigation was carried out through systematic electronic structure calculations within the framework of density functional theory (DFT) formalism. In our DFT modeling, we primarily highlighted the correlation between adsorption characteristics and the corresponding charge transfer mechanism for the sorbent and adsorbate along with the adsorbate induced work function change, which are immensely instrumental fundamental parameters for any surface investigation. We analyzed the electronic density of states (DOS) of the composite ( $\text{CO}_2$  adsorbed on the LSNs) as well as the individual systems after and before the adsorption process to elucidate the salient features of the electronic structures, as depicted in Fig. 8. The middle panel of Fig. 8a illustrates the total DOS of  $\text{Li}_4\text{SiO}_4$  before  $\text{CO}_2$  adsorption, exhibiting a wide bandgap semiconducting nature. But as soon as  $\text{CO}_2$  gets adsorbed on top of the LSNs, finite states are found to emerge near the Fermi level ( $E_F$ ) due to the interaction between  $\text{Li}_4\text{SiO}_4$  and the  $\text{CO}_2$  molecule, as shown in the top panel of Fig. 8a. Interestingly, we observed that the density of states corresponding to an isolated  $\text{CO}_2$  molecule (as depicted in the bottom panel of Fig. 8a) has been shifted substantially in the vicinity of  $E_F$  under the

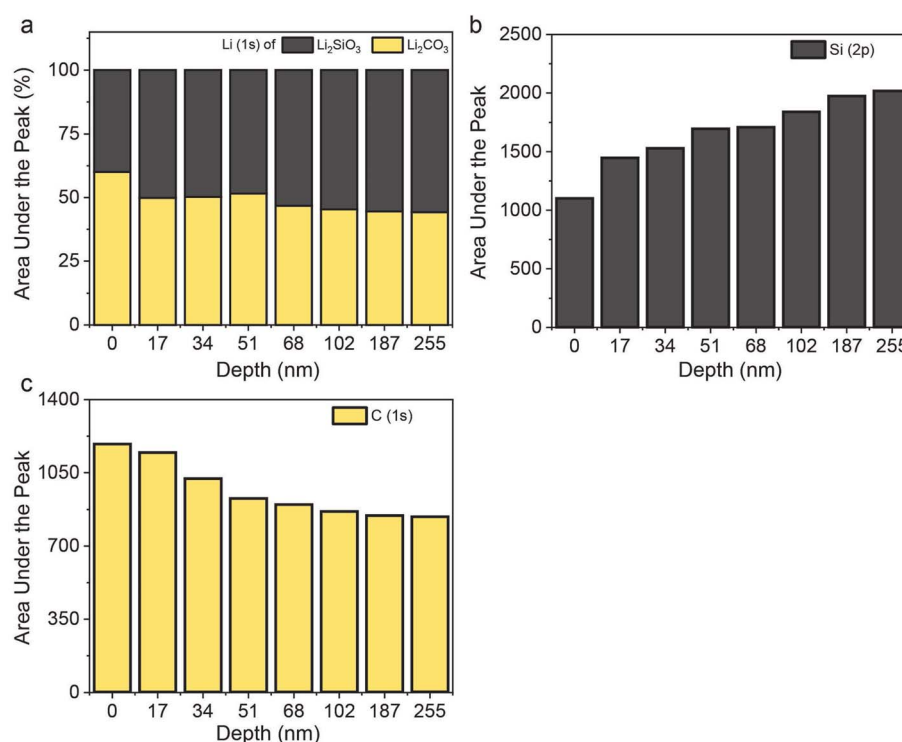
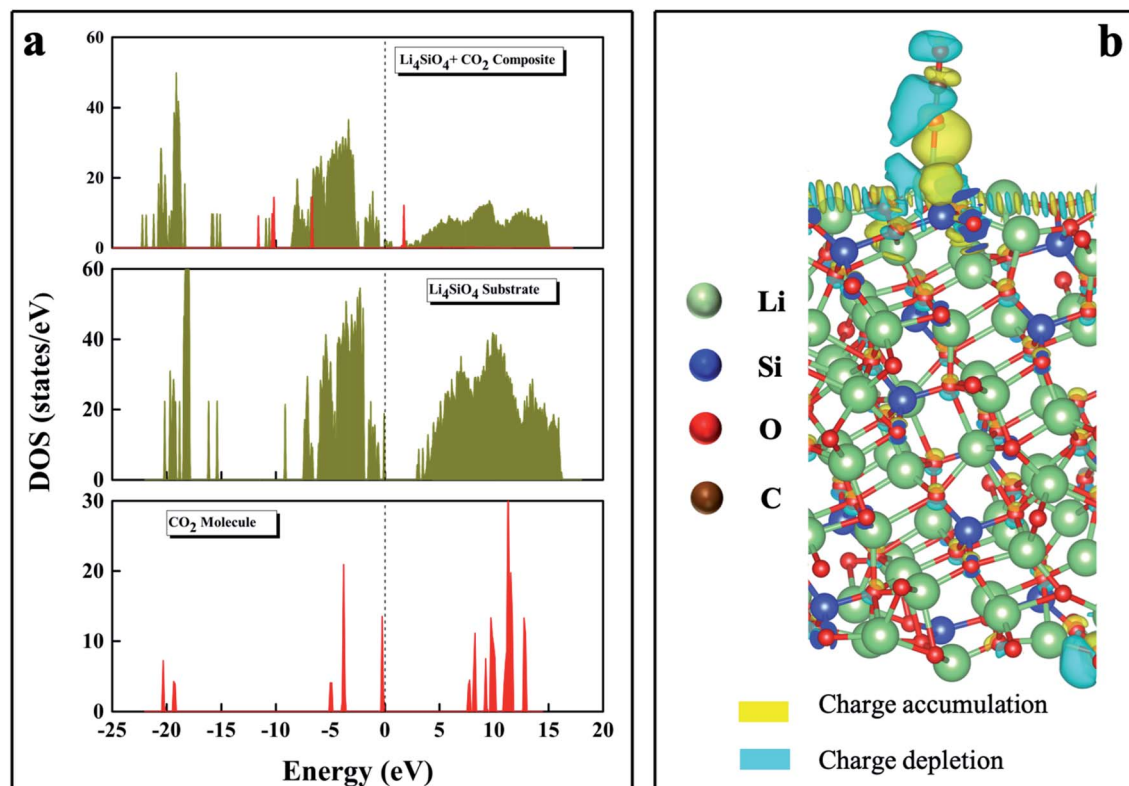


Fig. 7 Area under the peak of (a) Li 1s for  $\text{Li}_2\text{SiO}_3$  and  $\text{Li}_2\text{CO}_3$ , and (b) Si 2p and (c) C 1s of the LSN sample in the  $\text{CO}_2$  adsorbed state, from XPS fitting (Fig. S13†) at different etching depths.





**Fig. 8** (a) Density of states plot for CO<sub>2</sub> adsorbed on top of Li<sub>4</sub>SiO<sub>4</sub>. The top panel illustrates the total DOS of the composite systems after adsorption, while the middle and bottom panels represent the DOS of the isolated Li<sub>4</sub>SiO<sub>4</sub> sorbent and CO<sub>2</sub> molecule before adsorption. (b) Charge density distribution between a Li<sub>4</sub>SiO<sub>4</sub> nanosheet and CO<sub>2</sub> molecule. The accumulation and depletion of charge are denoted by yellow and blue color, respectively. The iso-surface value was set to 0.0003 e<sup>-</sup> Å<sup>-3</sup>. (c) Work function and DFT total energies in the bulk form of reactants and products.

influence of the LSN surface, which is also manifested through the charge transfer mechanism representation in the subsequent section. It is worth mentioning that we observed the finite density of states appear near the Fermi region after adsorption in the composite system. This reveals the fact that the adsorbate in the form of CO<sub>2</sub> is tuning the bandgap of the surface, which is Li<sub>4</sub>SiO<sub>4</sub>, which has also been reflected in the substantial charge transfer process. As we investigated the interaction of an incoming CO<sub>2</sub> with the Li<sub>4</sub>SiO<sub>4</sub> surface, the noticeable change in the electronic structure through the appearance of finite states after adsorption signifies the fact that CO<sub>2</sub> is chemisorbed on the Li<sub>4</sub>SiO<sub>4</sub> surface. The composite system represents the left-hand side of the reaction mechanism of CO<sub>2</sub> adsorption by Li<sub>4</sub>SiO<sub>4</sub> before converting to the product form, while our

theoretical analysis focused on the surface adsorption, whereas in the experimental section, the CO<sub>2</sub> adsorption occurred within the nanosheets of Li<sub>4</sub>SiO<sub>4</sub>.

The charge density distribution is illustrated in Fig. 8b, where it is observed that the charge is mainly accumulated around the Li-O bond region, indicating a valuable observation and validation of this work, as reflected in the covalent bond formation between the LSN surface and CO<sub>2</sub>. This particular theoretical finding has shed light not only on the CO<sub>2</sub> capture but also on the subsequent desorption possibility, as found in the experimental outcome. Bader charge analysis indicates that 0.85 e<sup>-</sup> Å<sup>-3</sup> (amount of charge) is transferred from a Li atom of LSNs to an O atom of CO<sub>2</sub> during the adsorption process. During the electron transfer process from the Li atom to the O

atom of  $\text{CO}_2$ , covalent bond formation occurred, which eventually helps in the  $\text{CO}_2$  adsorption/capture. This particular covalent bond formation also supports the adsorption/desorption process, as desorption would be favorable in the absence of a strong ionic bond between the surface and adsorbate. This is due to the higher electronegativity of oxygen atoms as compared to lithium and carbon, as both of them share their electrons with oxygen, which leads to charge depletion around the lithium and carbon atoms.

The work function values (Fig. 8c) for  $\text{Li}_2\text{SiO}_3$  and  $\text{Li}_2\text{CO}_3$  are higher as compared to those of both LSNs and LSN- $\text{CO}_2$  composite systems, suggesting that a larger amount of energy is required to extract an electron from  $\text{Li}_2\text{SiO}_3$  and  $\text{Li}_2\text{CO}_3$  surfaces as compared to the  $\text{Li}_4\text{SiO}_4$  system. Therefore, we could infer the favorable capture of a  $\text{CO}_2$  molecule by the LSNs, while the subsequent desorption of  $\text{CO}_2$  had been reflected in the previously discussed Bader charge analysis. This observation has also been verified theoretically from the reaction energy value of the reaction ( $\text{Li}_4\text{SiO}_4 + \text{CO}_2 \rightleftharpoons \text{Li}_2\text{SiO}_3 + \text{Li}_2\text{CO}_3$ ), which has been calculated as  $-1.36$  eV from DFT total energy calculations. Here, the negative reaction energy signifies the exothermic, spontaneous  $\text{CO}_2$  capture process. Thus, we have theoretically validated the experimental observation of not only the  $\text{CO}_2$  capture process but also the  $\text{CO}_2$  desorption. The adsorption of  $\text{CO}_2$  has also been confirmed from the elongated C–O bond being closer to the LSN surface as compared to that in the pre-adsorbed state, while the corresponding adsorption energy is found to be  $-1.54$  eV.

The cycling stability of the sorbents is determined by the efficiency of  $\text{CO}_2$  desorption, which is known to be difficult from an interior (core) portion of the double-shell model in conventional lithium silicates, causing a reduction in  $\text{CO}_2$  capture performances with every cycle for reported lithium silicates (Fig. 3b).<sup>5</sup> In addition to the formation of thick carbonate shells, the sintering of sorbent particles was another reason for the fast decline in capture capacity and kinetics in conventional silicates.<sup>8,9</sup> In the LSN sorbent, due to the absence of any carbonate shell,  $\text{CO}_2$  desorption was very efficient (nearly 100%, Fig. 3a). This allowed efficient regeneration and reuse of the LSNs, and even after 200 cycles, they remained active, without even a minute loss of  $\text{CO}_2$  capture capacity or kinetics. Also, although the sheets of LSNs have nano-dimensions, they are stacked and their overall particle size is in microns, making them sinter-proof and stable. Thus, the LSN sorbent neither generated the carbonate shell nor underwent sintering. This made  $\text{CO}_2$  adsorption–desorption a completely reversible process and hence the LSNs were stable and recyclable even after 200 cycles.

## Conclusions

In this work, we synthesized lithium silicate nanosheets by solid-state thermal treatment of DFNS and lithium nitrate. The LSNs showed  $\text{CO}_2$  capture capacity close to the theoretical value, with a high rate of  $\text{CO}_2$  adsorption. The nanosheet morphology of the LSNs provided a good external surface for efficient  $\text{CO}_2$  interaction with every Li-site, yielding high  $\text{CO}_2$  capture capacity (35.3 wt%  $\text{CO}_2$  using 60%  $\text{CO}_2$  feed gas). The

rate of  $\text{CO}_2$  capture is generally limited by the diffusion of  $\text{CO}_2$  and  $\text{Li}^+$  through the external carbonate shell, but since no such shell was formed in the LSNs, they showed extremely fast  $\text{CO}_2$  capture kinetics ( $0.22 \text{ g g}^{-1} \text{ min}^{-1}$ ). Notably, the LSNs show dramatic stability (even after 200 cycles without any loss in their capture capacity or kinetics), as compared to reported sorbents, which are known to systematically lose their capture capacity significantly. The LSN sorbent neither formed a carbonate shell nor underwent sintering, causing efficient adsorption–desorption with no loss in capture performance. Thus, the LSNs have all three desirable properties (high capture capacity, fast kinetics and cycling stability for more than 200 cycles) of a  $\text{CO}_2$  sorbent. Various kinetics and spectroscopic studies (XPD depth profiling and *in situ* DRIFT) were performed to prove the proposed mechanism of the mixed-phase model, which explained the unique  $\text{CO}_2$  capture behavior of lithium silicate nanosheets in terms of good capture kinetics and prolonged stability.

## Conflicts of interest

There are no conflicts to declare.

## Acknowledgements

This work was supported by the Department of Atomic Energy (DAE), Government of India (under project no. R&D-TIFR-RTI4003). We acknowledge the use of the EM and XRD facilities of TIFR, Mumbai.

## References

- 1 H. Yang, Z. Xu, M. Fan, R. Gupta, R. B. Slimane, A. E. Bland and I. Wright, Progress in carbon dioxide separation and capture: a review, *J. Environ. Sci.*, 2008, **20**, 14–27.
- 2 J. G. Vitillo, B. Smit and L. Gagliardi, Introduction: Carbon capture and separation, *Chem. Rev.*, 2017, **117**, 9521–9523.
- 3 V. O. Özçelik, K. Gong and C. E. White, Highly surface-active  $\text{Ca}(\text{OH})_2$  monolayer as a  $\text{CO}_2$  capture material, *Nano Lett.*, 2018, **18**, 1786–1793.
- 4 M. Bui, *et al.*, Carbon capture and storage (CCS): the way forward, *Energy Environ. Sci.*, 2018, **11**, 1062–1176.
- 5 Y. Zhang, Y. Gao, H. Pfeiffer, B. Louis, L. Sun, D. O'Hare and Q. Wang, Recent advances in lithium containing ceramic based sorbents for high-temperature  $\text{CO}_2$  capture, *J. Mater. Chem. A*, 2019, **7**, 7962–8005.
- 6 Y. Hu, W. Liu, Y. Yang, M. Qu and H. Li,  $\text{CO}_2$  capture by  $\text{Li}_4\text{SiO}_4$  sorbents and their applications: current developments and new trends, *Chem. Eng. J.*, 2019, **359**, 604–625.
- 7 M. Kato, S. Yoshikawa and K. Nakagawa, Carbon dioxide absorption by lithium orthosilicate in a wide range of temperature and carbon dioxide concentrations, *J. Mater. Sci. Lett.*, 2002, **21**, 485–487.
- 8 A. Nambo, J. He, T. Q. Nguyen, V. Atla, T. Druffel and M. Sunkara, Ultrafast carbon dioxide sorption kinetics



using lithium silicate nanowires, *Nano Lett.*, 2017, **17**, 3327–3333.

9 M. Z. Akram, V. Atla, A. Nambo, B. P. Ajayi, J. B. Jasinski, J. He, J. R. Gong and M. Sunkara, Low-temperature and fast kinetics for  $\text{CO}_2$  sorption using  $\text{Li}_6\text{WO}_6$  nanowires, *Nano Lett.*, 2018, **18**, 4891–4899.

10 A. K. Mishra, R. Belgamwar, R. Jana, A. Datta and V. Polshettiwar, Defects in nanosilica catalytically convert  $\text{CO}_2$  to methane without any metal and ligand, *Proc. Natl. Acad. Sci. U. S. A.*, 2020, **24**, 6383–6390.

11 M. Dhiman, A. Maity, A. Das, R. Belgamwar, B. Chalke, Y. Lee, K. Sim, J.-W. Nam and V. Polshettiwar, Plasmonic colloidosomes of black gold for solar energy harvesting and hotspots directed catalysis for  $\text{CO}_2$  to fuel conversion, *Chem. Sci.*, 2019, **10**, 6594–6603.

12 A. Maity, R. Belgamwar and V. Polshettiwar, Facile synthesis protocol to tune size, textural properties and fiber density of dendritic fibrous nanosilica (DFNS): Applications in catalysis and  $\text{CO}_2$  capture, *Nat. Protoc.*, 2019, **14**, 2177–2204.

13 A. Maity, S. Chaudhari, J. J. Titman and V. Polshettiwar, Catalytic nanosponges of acidic aluminosilicates for plastic degradation and  $\text{CO}_2$  to fuel conversion, *Nat. Commun.*, 2020, **11**, 3828.

14 P. V. Korake and A. G. Gaikwad, Capture of carbon dioxide over porous solid adsorbents lithium silicate, lithium aluminate and magnesium aluminate at pre-combustion temperatures, *Front. Chem. Eng.*, 2011, **5**, 215–226.

15 J. F. Moulder, W. F. Stickle, P. E. Sobol and K. D. Bomben, *Handbook of X-ray photoelectron spectroscopy*, ed. J. Chastain, Perkin-Elmer Corporation Physical Electronics Division, 1992, pp. 34–35.

16 A. Kaur, P. Chahal and T. Hogan, Selective Fabrication of SiC/Si Diodes by Excimer Laser under Ambient Conditions, *IEEE Electron Device Lett.*, 2016, **37**, 142–145.

17 H. Kim, H. D. Jang and M. Choi, Facile synthesis of macroporous  $\text{Li}_4\text{SiO}_4$  with remarkably enhanced  $\text{CO}_2$  adsorption kinetics, *Chem. Eng. J.*, 2015, **280**, 132–137.

18 M. T. Izquierdo, A. Turan, S. Garcia and M. M. Maroto-Valer, Optimization of  $\text{Li}_4\text{SiO}_4$  synthesis conditions by a solid state method for maximum  $\text{CO}_2$  capture at high temperature, *J. Mater. Chem. A*, 2018, **6**, 3249–3257.

19 P. V. Subha, B. N. Nair, P. Hareesh, A. P. Mohamed, T. Yamaguchi, K. G. K. Warrier and U. S. Hareesh, Enhanced  $\text{CO}_2$  absorption kinetics in lithium silicate platelets synthesized by a sol-gel approach, *J. Mater. Chem. A*, 2014, **2**, 12792–12798.

20 P. V. Subha, B. N. Nair, A. P. Mohamed, G. M. Anilkumar, K. G. K. Warrier, T. Yamaguchi and U. S. Hareesh, Morphologically and compositionally tuned lithium silicate nanorods as high-performance carbon dioxide sorbents, *J. Mater. Chem. A*, 2016, **4**, 16928–16935.

21 N. A. Zubbri, A. R. Mohamed and M. Mohammadi, Parametric study and effect of calcination and carbonation conditions on the  $\text{CO}_2$  capture performance of lithium orthosilicate sorbent, *Chin. J. Chem. Eng.*, 2018, **26**, 631–641.

22 K. Wang, X. Wang, P. Zhao and X. Guo, High-temperature capture of  $\text{CO}_2$  on lithium based sorbents prepared by a water-based sol-gel technique, *Chem. Eng. Technol.*, 2014, **37**, 1552–1558.

23 M. E. Bretado, V. Guzman Velderrain, D. Lardizabal Gutierrez, V. Collins-Martinez and A. L. Ortiz, A new synthesis route to  $\text{Li}_4\text{SiO}_4$  as  $\text{CO}_2$  catalytic/sorbent, *Catal. Today*, 2005, **4**, 863–867.

24 L. Ortiz, M. A. E. Bretado, V. G. Velderrain, M. M. Zaragoza, J. S. Gutierrez, D. L. Gutierrez and V. Collins-Martinez, Experimental and modeling kinetic study of the  $\text{CO}_2$  absorption by  $\text{Li}_4\text{SiO}_4$ , *Int. J. Hydrogen Energy*, 2014, **39**, 16656–16666.

25 S. Shan, S. Li, Q. Jia, L. Jiang, Y. Wang and J. Peng, Impregnation precipitation preparation and kinetic analysis of  $\text{Li}_4\text{SiO}_4$ -based sorbents with fast  $\text{CO}_2$  adsorption rate, *Ind. Eng. Chem. Res.*, 2013, **52**, 6941–6945.

26 X. Yang, W. Liu, J. Sun, Y. Hu, W. Wang, H. Chen, Y. Zhang, X. Li and M. Xu, Preparation of novel  $\text{Li}_4\text{SiO}_4$  sorbents with superior performance at low  $\text{CO}_2$  concentration, *ChemSusChem*, 2016, **9**, 1607–1613.

27 Y. Hu, W. Liu, Y. Yang, X. Tong, Q. Chen and Z. Zhou, Synthesis of highly efficient, structurally improved  $\text{Li}_4\text{SiO}_4$  sorbents for high-temperature  $\text{CO}_2$  capture, *Ceram. Int.*, 2018, **44**, 16668–16677.

28 G. J. Rao, R. Mazumder, S. Bhattacharyya and P. Chaudhuri, Synthesis,  $\text{CO}_2$  absorption property and densification of  $\text{Li}_4\text{SiO}_4$  powder by glycine-nitrate solution combustion method and its comparison with solid state method, *J. Alloys Compd.*, 2017, **725**, 461–471.

29 Y. Hu, W. Liu, Z. Zhou and Y. Yang, Preparation of  $\text{Li}_4\text{SiO}_4$  sorbents for carbon dioxide capture via a spray-drying technique, *Energy Fuels*, 2018, **32**, 4521–4527.

30 J. A. Lercher, C. Colombier and H. Noller, Acid-base properties of alumina-magnesia mixed oxides. Part 4. Infrared study of adsorption of carbon dioxide, *J. Chem. Soc., Faraday Trans. 1*, 1984, **80**, 949–959.

31 M. L. Grasso, P. Arneodo Laroche and F. C. Gennari,  $\text{CO}_2$  capture properties of  $\text{Li}_4\text{SiO}_4$  after aging in air at room temperature, *J. CO<sub>2</sub> Util.*, 2020, **38**, 232–240.

32 K. Coenen, F. Gallucci, B. Mezari, E. Hensen and M. V. Annaland, An *in situ* IR study on the adsorption of  $\text{CO}_2$  and  $\text{H}_2\text{O}$  on hydrotalcites, *J. CO<sub>2</sub> Util.*, 2018, **24**, 228–239.

